Particuology 11 (2013) 41–47

Contents lists available at SciVerse ScienceDirect

Particuology

journal homepage: www.elsevier.com/locate/partic

Variability of SO_2 in an intensive fog in North China Plain: Evidence of high solubility of SO_2

Qiang Zhang[a], Xuexi Tie[b,c,*], Weili Lin[d], Junji Cao[b], Jiannong Quan[a], Liang Ran[e], Wanyun Xu[e]

[a] Beijing Weather Modification Office, Beijing, China
[b] Key Laboratory of Aerosol, SKLLQG, Institute of Earth Environment, Chinese Academy of Sciences, Xi'an, China
[c] National Center for Atmospheric Research, Boulder, CO, USA
[d] Chinese Academy of Meteorological Science, Beijing, China
[e] Department of Atmospheric and Oceanic Sciences, School of Physics, Peking University, Beijing, China

ARTICLE INFO

Article history:
Received 29 January 2012
Received in revised form 27 August 2012
Accepted 12 September 2012

Keywords:
Solubility of SO_2
Fogs in the North China Plain
Aqueous phase reactions

ABSTRACT

A field experiment was conducted in an intensive fog event between November 5 and November 8, 2009, in a heavily SO_2-polluted area in North China Plain (NCP), to measure SO_2 and other air pollutants, liquid water content (LWC) of fog droplets, and other basic meteorological parameters. During the fog period, the concentrations of SO_2 showed large variability, which was closely related to the LWC in the fog droplets. The averaged concentration of SO_2 during non-fog periods was about 25 ppbv, while during the fog period, it rapidly reduced to about 4–7 ppbv. Such large reduction of SO_2 suggested that a majority of SO_2 (about 70%–80%) had reverted from gas to aqueous phase on account of the high solubility of SO_2 in water in the fog droplets. However, the calculated gas to aqueous phase conversion was largely underestimated by merely using the Henry's Law constant of SO_2, thus suggesting that aqueous reaction of SO_2 in fog droplets might play some important role in enhancing the solubility of SO_2. To simplify the phenomenon, an "effective solubility coefficient" is proposed in this study. This variability of SO_2 measurement during the extensive fog event provides direct evidence of oxidation of SO_2 in fog droplets, thus providing important implications for better understanding of the acidity in clouds, precipitation, and fogs in NCP, now a central environmental focus in China due to its rapid economic development.

© 2012 Chinese Society of Particuology and Institute of Process Engineering, Chinese Academy of Sciences. Published by Elsevier B.V. All rights reserved.

1. Introduction

Sulfur dioxide (SO_2) is released to the atmosphere through both natural and anthropogenic emissions. Natural emissions include volcanic eruptions and biomass burnings. Anthropogenic emissions are mainly due to coal and oil burning, which accounts for more than 75% of global emissions (Chin, Rood, Lin, Müller, & Thompson, 2000). Coal combustion accounts for about 70% of China's total energy consumption, increasing rapidly in recent years due to significant economical development in China to 2.01 billion metric tons in 2009 (IEA, 2010), which leads to high SO_2 emissions (Kawamoto, Hayasaka, Nakajima, Streets, & Woo, 2004; Streets & Waldhoff, 2000). One of the major fates of gaseous SO_2 is to form sulfate particles. Understanding the formation of sulfate particles in the troposphere is critical due to their effects on human health and climate (Malm, Trijonis, Sisler, Pitchford, & Dennis, 1994; Pandey, Kumar, & Devotta, 2005; Tie, Wu, & Brasseur, 2009; Zhao, Tie, & Lin, 2006). Thus, the study of SO_2 budget (such as its emission, transformation, and deposition) has become a crucial environmental issue in China.

There were several studies regarding the effect of sulfate particles on acidity of cloud in the North China Plain (NCP) region. For example, Zhou et al. (2009) showed that the oxidation of SO_2 was twice as high in summer as in winter. Wang et al. (2011) suggested that the concentrations of SO_2 were extremely high in NCP, and its scavenging rate was faster than some other soluble aerosol particles (such as Ca^{2+} and Na^{+}), leading to important effect on the acidity in clouds. The main focus of this study will be on the solubility of SO_2, which is a very important parameter in numerical models.

Sulfur dioxide is a gas soluble in water, and can be oxidized within cloud and fog droplets, producing sulfuric acid (Dutkiewicz, Burkhard, & Husain, 1995; Hoag, Collett, & Pandis,

Abbreviations: a.s.l, above sea level; GtA, gas to aqueous; LWC, liquid water content; MODIS, MODerate resolution Imaging Spectroradiometer; NCP, North China Plain; SCIAMACHY, SCanning Imaging Absorption spectroMeter for Atmospheric CartograpHY; SMPS, scanning mobility particle sizer; VIS, visibility; WMO, world meteorological organization.

* Corresponding author at: National Center for Atmospheric Research, Boulder, CO, USA. Tel.: +1 303 497 1470; fax: +1 303 497 1400.
E-mail addresses: xxtie@ucar.edu, tiexx@ieecas.cn (X. Tie).

1674-2001/$ – see front matter © 2012 Chinese Society of Particuology and Institute of Process Engineering, Chinese Academy of Sciences. Published by Elsevier B.V. All rights reserved.
http://dx.doi.org/10.1016/j.partic.2012.09.005

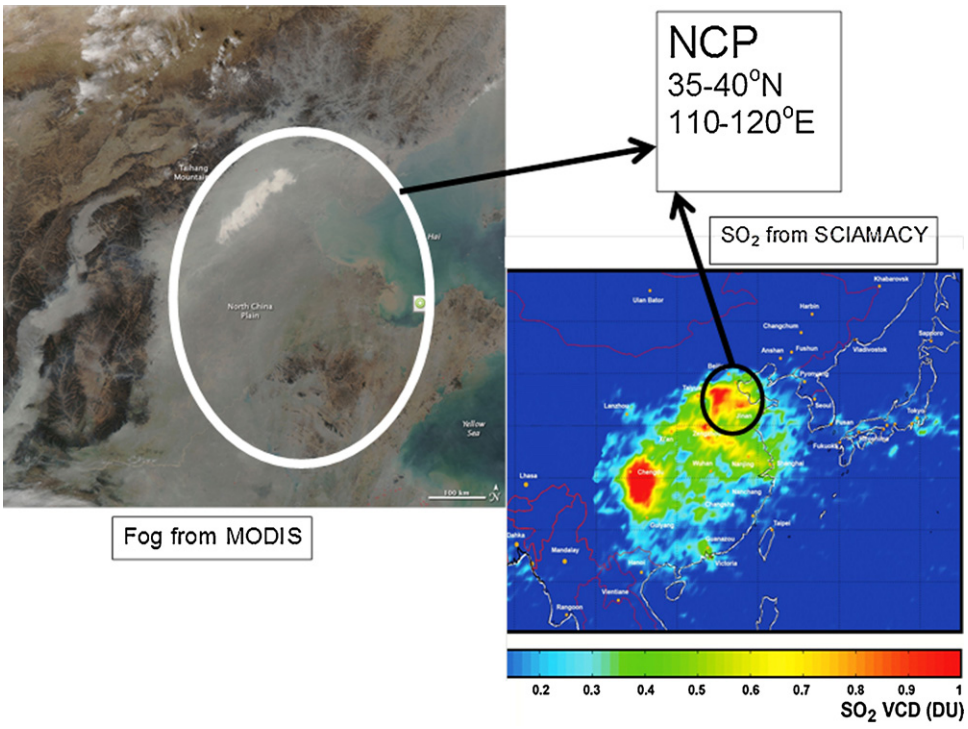

Fig. 1. Horizontal distribution of SO_2 concentrations (averaged from 2003 to 2008) measured by satellite SCIAMACY (right panel), and horizontal distribution of fogs measured by satellite MODIS, on November 6, 2009 (left panel). Circles show the location of the NCP region.

1999; Kreidenweis et al., 2003). In this study, a field experiment was conducted in a heavily SO_2-polluted area located in NCP. During the experiment, SO_2 and other air pollutants, liquid water content (LWC) of fog droplets, and basic meteorological parameters were measured. A large variability of SO_2 and LWC of fog droplets were observed, providing a good opportunity to study the SO_2 conversion between gas phase and aqueous phase. The study has important implications for understanding the aqueous oxidation of SO_2 in fog droplets, which significantly influences the acidity of fogs. The acidity in clouds, precipitation, and fogs is a central environmental focus in China due to her rapid economic development, and the study can provide important information for the environmental issues in the NCP region.

In Section 2 of this paper we describe the field experiment, including instruments and data. In Section 3, we analyze the result of the experiment to study the solubility of SO_2 in fog droplets.

2. Description of experiment

2.1. Information of the experiment

The field experiment took place at the Wuqing Meteorological Station (39°23′N, 117°1′E, 7.4 m a.s.l.) in Tianjin. The measurement site is about 30 km away from the center of Tianjin (Fig. 1), which is a mega city with a population of 10 million. During recent years, the rapid increase of economical development resulted in heavy atmospheric pollution, especially SO_2 pollution, in this region (Tie & Cao, 2009; Zhang, Ma, Tie, Huang, & Zhao, 2009).

Fig. 1 shows the horizontal distribution of SO_2 concentrations measured by satellite SCIAMACHY (SCanning Imaging Absorption spectroMeter for Atmospheric CartograpHY), and the horizontal distribution of fogs measured by satellite MODIS (Moderate Resolution Imaging Spectroradiometer), indicating that fog formation is closely related to the high concentration of SO_2 in the NCP region. The coherence between high SO_2 concentrations and frequent fog formation provides a good opportunity to study SO_2 solubility by analyzing in situ measurements of SO_2 concentrations and fog droplets in the NCP region. Intensive field measurement was conducted during a period of the fog season (between November 5 and November 8, 2009) to study the variability of SO_2 and its correlation to liquid water content (LWC) during the formation of fogs. Several instruments were deployed during the field experiment, the detailed information of which is listed in Table 1. These integrated instruments provide necessary information to study the solubility of SO_2 in fog droplets. To ensure the quality of measurements (QA/QC issue), all the instruments were calibrated before measurement. More detailed information of the instruments was described by Zhang et al. (2009) and Quan et al. (2011).

2.2. Background of meteorological conditions during experiment

An intensive fog event occurred between November 5 and November 8, 2009, in the NCP region, during which, the region was

Table 1
List of instruments used in field experiment.

Instrument	Purpose/comment	Range/detection limit/accuracy
DMT FM-100	Fog droplet spectra	2–32 μm
TSI SMPS (DMA, Model 3081; CPC, Model 3772)	Aerosol concentration, spectra	10–662 nm
TEI Model 49i	O_3 concentration	0.5 ppbv
TEI Model 42iTL	NO–NO_2–NO_x concentration	0.025 ppbv
TEI Model 43CTL	SO_2 concentration	0.05 ppbv
TEI Model 48C	CO concentration	0.04 ppmv
Vaisala PWD-20	Visibility	10–20000 m
Vaisala WTX-510	RH, T, wind, pressure	3% RH, 0.3 °C, 0.3 m/s, 0.5 Pa

DMT: droplet measurement technologies; SMPS: scanning mobility particle sizer; TEI: thermo environmental instruments.

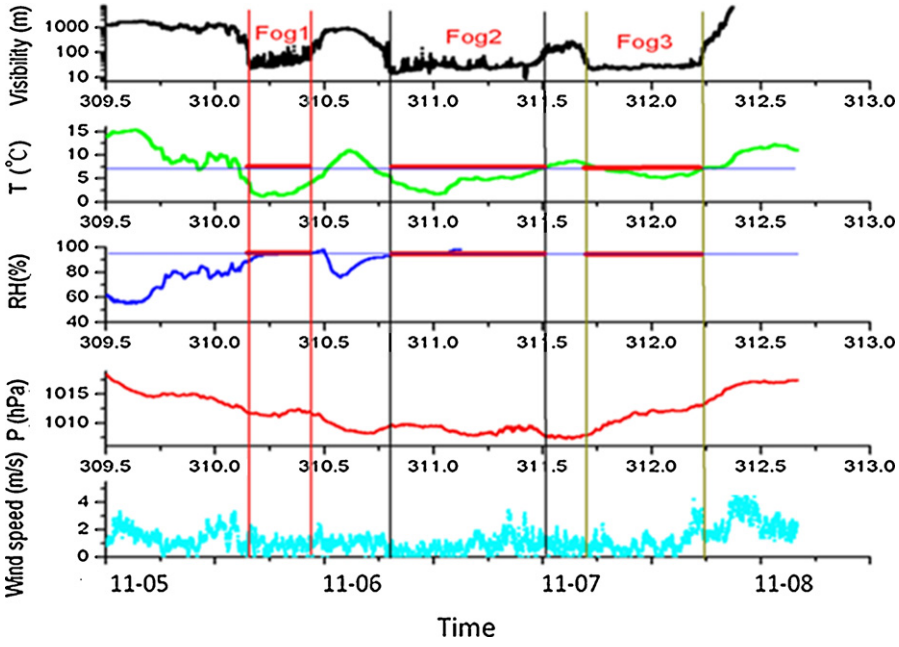

Fig. 2. Detailed evolution of meteorological conditions (visibility, temperature, relative humidity (RH), surface pressure and wind speed) during the fog formation period (between November 5 to November 8). The RH data from November 7, 4:38 to November 8, 8:54 cannot be used due to interference of liquid fog water on the RH instrument. The thick red lines indicate the occurrence of fog events. (For interpretation of the references to color in this figure legend, the reader is referred to the web version of this article.)

under the effect of a weak low-pressure system, with calm winds. The detailed evolution of the meteorological conditions (such as visibility, temperature, relative humidity (RH), surface pressure and wind speeds), is described in Fig. 2, showing that the averaged surface wind speed was only 1.1 m/s during the event, especially from late November 5 to early November 8. The averaged surface temperature was low (6.8 °C) and humidity was high with large variations, exceeding or equal to 100% after late November 5. These weather and meteorological conditions were very favorable for fog formation. After the fog event (late on November 8, 2009), the low-pressure system moved out of the NCP region. As a result, the averaged surface wind speed rapidly increased to about 4 m/s, and the averaged surface temperature increased to about 15 °C.

Fig. 3 shows the measured aerosol number concentrations during the fog event — very high, with a maximum of ~10,000 particles/cm^3, suggesting that the fog event was accompanied by high aerosol pollution. For relatively larger particles (diameters > 100 nm), which had higher concentrations than the smaller particles, they should have the highest impact on visibility. However, the variability of the larger particles was not consistent with the variation of visibility, indicating that the extremely low visibility was not caused by aerosol particles.

During the fog event, repeated formation of fog occurred. Based on the duration of fog occurrences in the event, three fog periods are defined according to the combined characteristics of observed relative humidity (RH), ambient temperature (*T*), fog LWC, and the range of visibility (VIS). The first fog period (Fog-1) occurred from 3:45 to 10:42 (LT), November 6. The second fog period (Fog-2) appeared from 19:10, November 6 to 12:27, November 7, and the third fog period (Fog-3) occurred from 16:29, November 7 to 5:40, November 8 (see Fig. 4). Fog event is defined by the conditions of visibility (VIS) and relative humidity (RH). Based on the criterion of world meteorological organization (WMO), fog occurrence is defined by the conditions: VIS < 1 km and RH ~ 100%. Another important indicator of fog occurrence is the appearance of liquid water content (LWC). According to the study of Quan et al. (2011), the fog event is defined by the citifications: LWC > 0.001 g/m^3 or VIS < 200 m, in this measurement. Detailed analysis of the effects of meteorological conditions and the criteria for the formation of fogs is shown in Quan et al. (2011).

3. Results and discussion

3.1. Measurement of air pollutants and fogs

One of the important indicators for the occurrence of fogs is atmospheric LWC. Measurement in Fig. 4 shows that liquid water appeared during all the 3 fog periods, with averaged LWC of 0.23,

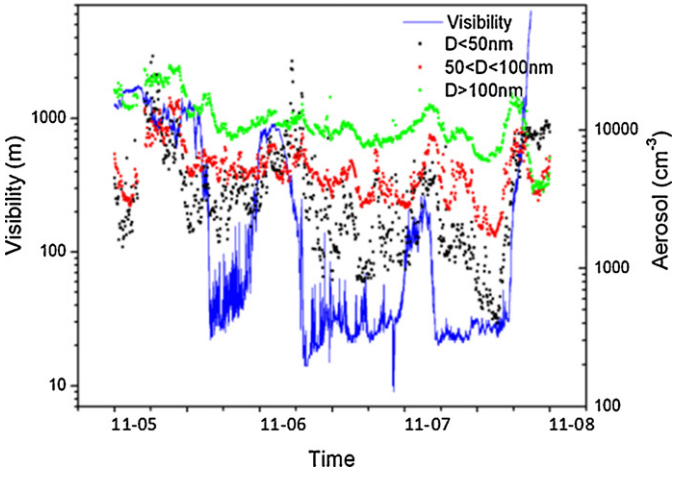

Fig. 3. Measured aerosol number concentrations during the fog event. Black dots represent fine particles (diameter < 50 nm); red dots represent particles with diameters between 50 and 100 nm; and green dots represent particles with diameters larger than 100 nm. The blue line shows the corresponding visibility. (For interpretation of the references to color in this figure legend, the reader is referred to the web version of this article.)

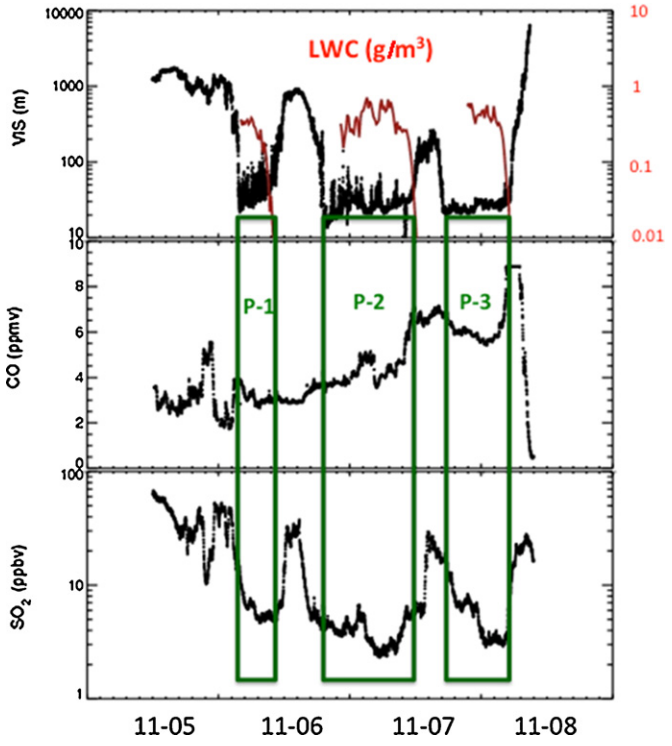

Fig. 4. Measured fog liquid water content (red lines in upper panel), the range of visibility (black lines in upper panel), concentration of CO (middle panel), and concentration of SO_2 (lower panel). The green boxes indicate the 3 fog periods. (For interpretation of the references to color in this figure legend, the reader is referred to the web version of this article.)

0.35, and 0.35 g/m^3. Fig. 4 also shows the variability of visibility, CO, and SO_2 before, during, and after the 3 fog appearances. Visibility decreased rapidly during fogging. The mean visibility range was about 870 m during the non-fog periods, which was relatively low, indicating that the concentrations of aerosols were high during the entire measurement (a heavy haze event). During the 3 fog periods, the visibility was reduced to the extremely low values of 20–50 m. Since extremely low visibility events were closely related to the formation of fogs, it could be used as an indicator for the occurrence of fogs in the NCP region. Measured SO_2 concentrations showed strong variability, closely related to the appearance of fogs and LWC, suggesting possible strong effects of LWC on the solubility of SO_2. The averaged concentration of SO_2 during the non-fog period was about 25 ppbv, while, in contrast, during the 3 fog periods it rapidly decreased to 6.8, 4.4, 7.2 ppbv, respectively. In order to better understand the causes of the large reduction in SO_2 concentrations during the fogs, the measured CO was analyzed (in the middle panel of Fig. 4). The main difference between CO and SO_2 is that CO is almost insoluble in water, while SO_2 is soluble. CO variations were not related to the occurrence of fogs or the LWC. The averaged concentration of CO during the non-fog period was 5.2 ppmv. Unlike SO_2, during the 3 fog periods, changes in CO concentrations were not significant, with mean values of 4.8, 5.9 and 7.6 ppmv, respectively. Because CO is not soluble, there was no large variability in its concentration. After the fog period, the averaged wind speed increased from 1.1 to 4.1 m/s, leading to a sharp decrease in CO concentration (from 10 to 2 ppmv in a few hours). The different behaviors between CO and SO_2 variations during the fog periods suggest that SO_2 was significantly reduced by dissolving gas-phase SO_2 in fog droplets during the formation of fogs.

Fig. 5 shows a quantitative analysis of the effect of fog water on SO_2 concentrations, indicating that during the 3 fog periods,

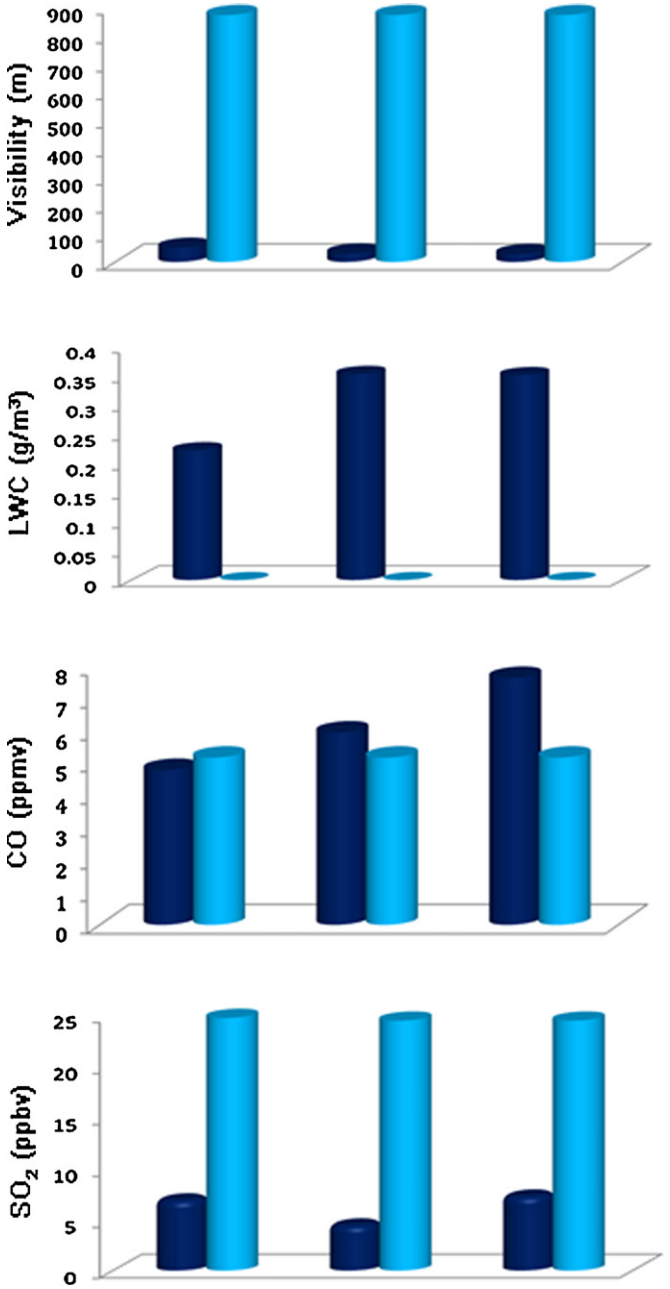

Fig. 5. Effects of fog formation on visibility (panel 1), LWC (panel 2), CO concentrations (panel 3), and SO_2 concentrations (panel 4). The dark blue columns show the mean values during the 3 fog periods, and the light blue columns show the mean values during non fog periods. (For interpretation of the references to color in this figure legend, the reader is referred to the web version of this article.)

visibility was reduced by 94%, 96%, and 96%, respectively. There were no consistent changes in CO concentrations, with −8%, +13%, and +46% variations during the 3 fog periods, respectively. In contrast, SO_2 concentrations were consistently reduced by −72%, −82%, and −71% during the 3 fog periods, respectively. The large reduction of gas-phase concentrations of SO_2 indicates that a majority of SO_2 (about 70%–80%) had been conveyed from gas phase to aqueous phase, that is, large conversion from gas-phase SO_2 to aqueous-phase of SO_2, thus verifying the high solubility of SO_2.

3.2. SO_2 solubility

The solubility of SO_2 is determined by an effective Henry's Law constant (H_{eff}) which accounts for both the effect of standard Henry's Law constant and the effect of dissociation. The effective Henry Law constant of SO_2 is expressed by the following formulas (Carmichael & Peters, 1979; Chameides, 1984):

$$SO_2(g) \leftrightarrow SO_2(aq) \quad (H_{SO_2})$$

where $SO_2(g)$ and $SO_2(aq)$ represent SO_2 concentrations in gas and aqueous phases, respectively. The standard Henry's Law constant of SO_2 (H_{SO_2}) is small (1.2 M/atm, at T = 298 K). However, SO_2 undergoes the following dissociation processes in droplets:

$$H_2O + SO_2(aq) \leftrightarrow HSO_3^- + H^+ \quad \text{(eq1)}$$

$$HSO_3^- \leftrightarrow SO_3^{2-} + H^+ \quad \text{(eq2)}$$

where the equilibrium constants for Eqs. (1) and (2) are shown in Seinfeld and Pandis (1998). As a result, the effective Henry's Law constant of SO_2 (H_{eff}) can be expressed as:

$$H_{eff} = H_{SO_2}\left(1 + eq1/\left[H^+\right]\left(1 + eq2/\left[H^+\right]\right)\right) \quad (1)$$

Eq. (1) indicates that the effective Henry's Law constant is strongly dependent on the acidity (or pH value) of droplets. The values of H_{eff} under different pH values are 2.2×10^1, 2.0×10^2, 2.0×10^3, 2.0×10^4 and 3.0×10^5 (M/atm), with pH values of 3.0, 4.0, 5.0, 6.0 and 7.0, respectively. These results suggest that pH values have important effect on the calculation of solubility of SO_2 in droplets. Thus, knowing the pH values at the measurement site is important. There were some studies on pH values in and near the measurement site. Tang, Xu, Ba, and Wang (2010) showed that the pH value in Tianjin ranges between 5.0 and 5.6 during the 2000–2006 period. Furthermore, their study suggested that the acidity in Tianjin increased from 2000 to 2006, with a rate of −0.25/year for the pH value. With linear interpolation, the pH values were estimated to range between 4.0 and 5.0 in 2009. There are also unpublished data (Yiyang Xie, Tianjin Meteorological Bureau, personal communication, 2009) showing pH values at the measurement site being 5.1 on October 25–26, 2007. Although these data provide useful information of the pH values at the measurement site, there is still large uncertainty due to lack of in situ measurements of pH values. However, based on the information shown above, the pH values are considered to likely lie between 4.0 and 6.0 at the measurement site. In this study, we use this wide range of pH values to conduct a series of sensitivity studies on the solubility of SO_2. Fig. 6 shows the calculated and measured gas-phase SO_2 concentrations during the fog period. The result indicates that the calculated gas to aqueous (GtA) phase conversion is underestimated with all the pH values (from 4.0 to 6.0), suggesting that the actual GtA conversion is larger than the calculated values with the application of the effective Henry's Law constant. In order to quantitatively highlight the underestimation of GtA by the calculation, Fig. 7 shows the averaged SO_2 concentrations with various pH values and comparison with measured values. The result shows that the calculated gas SO_2 concentrations range between 16 and 24 ppbv, contrasting the measured value of 5 ppbv. The highest underestimation occurs with the lowest pH value (400% with pH of 4), while the lowest underestimation with the highest pH value (80% with pH of 6). The sensitivity of the GtA conversion to different air temperature is also calculated, showing a large underestimation of GtA conversion for temperature ranging from 280 to 298 K. The above results show that the measured GtA conversion cannot be explained by using the effective Henry's Law constant in the calculation. Other processes might play important roles in controlling the solubility of SO_2, calling for careful study.

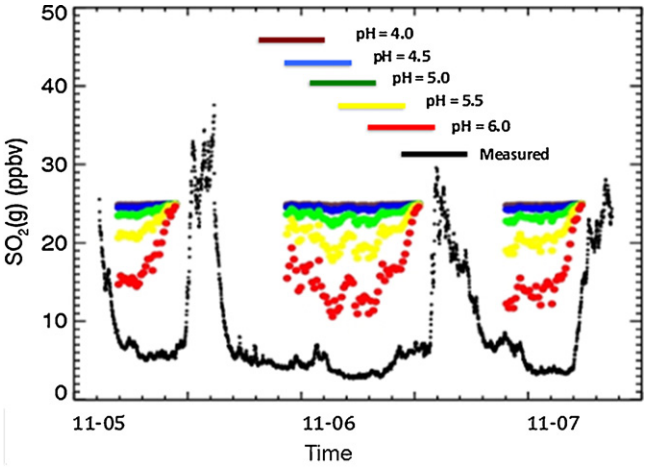

Fig. 6. Sensitivity study of the effect of pH values on gas to aqueous phase conversion of SO_2. The black line indicates the measured gas-phase concentrations of SO_2, and the color lines represent the calculated SO_2 concentration using the effective Henry's Law constants under different pH values. (For interpretation of the references to color in this figure legend, the reader is referred to the web version of this article.)

As suggested by Ravishankara (1997), the actual GtA conversion of chemical species in liquid water of clouds/fogs is determined by the following factors: (1) the standard Henry's Law constant, which is the first step to determine the solubility of chemical species; (2) the disassociation rate of a chemical species in droplets, which is a factor to enhance the solubility of chemical species; and (3) the rate of aqueous reaction of chemical species in droplets, which can further increase the GtA conversion or solubility of chemical species.

Fig. 8 provides a schematic description of the enhancement of solubility of SO_2 due to aqueous phase reactions, indicating that the effective Henry's Law constant combined with aqueous phase reactions can enhance the solubility of SO_2. In this study, we refer to this combined process as the "effective solubility". Fig. 8 shows that when SO_2 molecules penetrate into a liquid droplet, aqueous reactions convert SO_2 into other chemical species. As a result, more molecules of SO_2 can be transported into water droplets, and less molecules of SO_2 are returned back to the atmosphere, leading to the enhancement of the GtA conversion or the solubility of SO_2. The quantitative calculation of the solubility of SO_2 with the

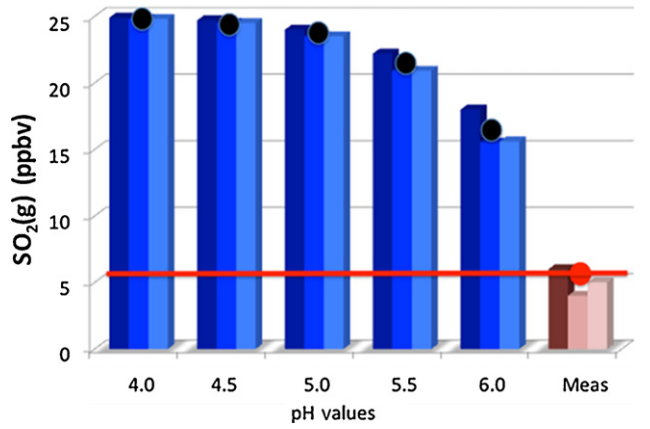

Fig. 7. Averaged gas-phase concentrations of SO_2 (blue bars) for the 3 fog periods, which are calculated by using the effective Henry's Law constant under different pH values. The brown-pink-light pink bars represent the measured average concentrations of SO_2 during the 3 fog periods. (For interpretation of the references to color in this figure legend, the reader is referred to the web version of this article.)

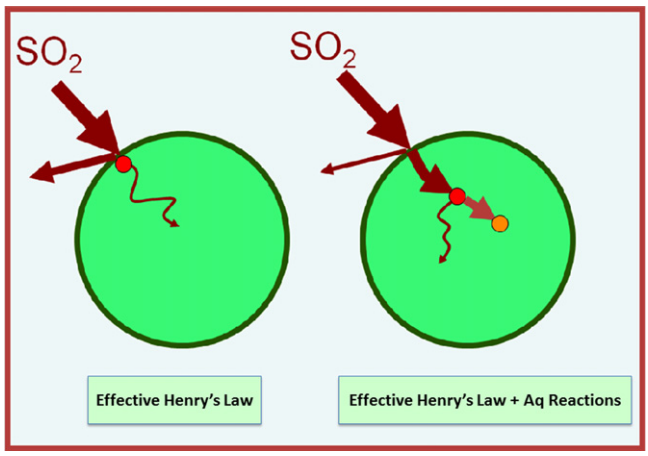

Fig. 8. Schematic description of enhancement of solubility of SO_2 due to aqueous phase reactions. Left panel shows processes which affect solubility of SO_2 without considering aqueous reactions. Right panel shows processes which affect the solubility of SO_2 with considering aqueous reactions, which lead to enhancement of the solubility of SO_2.

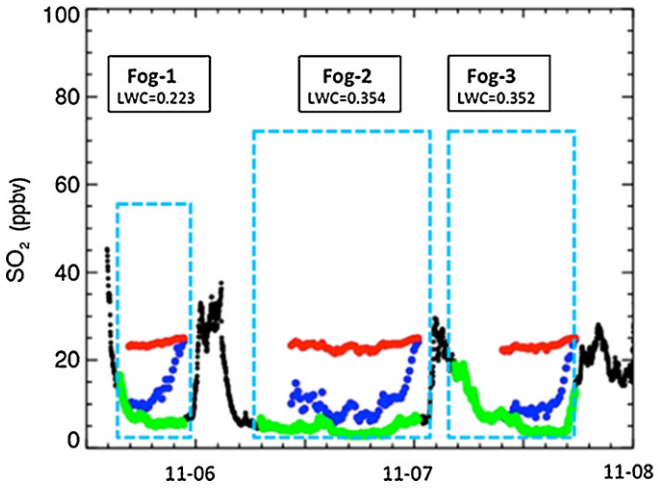

Fig. 9. Measured SO_2 concentrations (black lines during the non-fog periods, and green lines during the 3 fog periods), and calculated SO_2 concentrations (red lines: without considering the aqueous phase reactions; blue lines: with considering the aqueous phase reactions). (For interpretation of the references to color in this figure legend, the reader is referred to the web version of this article.)

consideration of aqueous phase reaction is described by the following method.

According to the study by Seinfeld and Pandis (1998), there are two important aqueous-phase reactions for SO_2. After SO_2 is dissolved in water, it can either react with H_2O_2 or O_3. Because O_3 is a very low-solubility species (with a Henry's Law constant of 0.02), the aqueous-phase reaction with O_3 is not significant as compared to reaction with H_2O_2. Thus, the calculation of solubility of SO_2 is mainly determined by the following expressions:

$$SO_2(g) \leftrightarrow SO_2(aq) \quad \text{(R-1)}$$

$$H_2O_2(g) \leftrightarrow H_2O_2(aq) \quad \text{(R-2)}$$

$$SO_2(aq) + H_2O_2(aq) \rightarrow H_2SO_4(aq) \quad \text{(R-3)}$$

$$O_3(g) \leftrightarrow O_3(aq) \quad \text{(R-4)}$$

$$SO_2(aq) + O_3(aq) \rightarrow H_2SO_4(aq) \quad \text{(R-5)}$$

where $H_2O_2(g)$ and $H_2O_2(aq)$ represent H_2O_2 concentrations for gas and aqueous phase, respectively; $O_3(g)$ and $O_3(aq)$ represent O_3 concentrations for gas and aqueous phase, respectively. These expressions suggest that the solubility of SO_2 depends on three quantities: (1) the aqueous concentrations of $SO_2(aq)$ in droplets, (2) the aqueous concentrations of $H_2O_2(aq)$ and $O_3(aq)$ in droplets, and (3) the rate of aqueous reactions (k) between $SO_2(aq)$ and $H_2O_2(aq)/O_3(aq)$. Because the rates of the aqueous reactions are very fast (Seinfeld & Pandis, 1998), it requires more $SO_2(g)$ to be converted to $SO_2(aq)$, and the value of $SO_2(aq)$ is strongly dependent upon the availability of $H_2O_2(aq)$ and $O_3(aq)$. As a result, the solubility of SO_2 is enhanced and the "effective solubility coefficient" (S_{eff}) of SO_2 can be expressed:

$$S_{eff}(SO_2) = \frac{[H_e(H_2O_2)H_2O_2(g) + H_e(O_3)O_3(g)]}{SO_2(g)} \quad (2)$$

where $S_{eff}(SO_2)$ represents the "effective solubility coefficient" of SO_2, $H_e(H_2O_2)$ and $H_e(O_3)$ represent the effective Henry's Law constants of H_2O_2 and O_3, respectively. Generally the term of $H_e(O_3)$ $O_3(g)$ is smaller than $H_e(H_2O_2)$ $H_2O_2(g)$, due to the high solubility of H_2O_2. Thus Eq. (2) can be simplified to:

$$S_{eff}(SO_2) = \frac{[H_e(H_2O_2)H_2O_2(g)]}{SO_2(g)} \quad (3)$$

The "effective solubility coefficient" is tested by comparing the calculation with measurements of the aqueous phase partitioning of SO_2 in fog droplets. For the calculation, the measured values of LWC are used (see Fig. 4). The initial values of SO_2 are set to be the measured values before the occurrences of the fogs. During the fog periods, the concentration of $SO_2(g)$ is set to be 5.0 ppbv which is similar to the measured SO_2 concentrations during the 3 fog periods, and the concentration of $H_2O_2(g)$ is set to be 1.0 ppbv which was often measured in the atmosphere (Ren et al., 2009). The concentrations O_3 is set be 30 ppbv which is similar to the measured O_3 concentrations. The pH and temperature are set to be 5.1 and 280 K respectively. With the above considerations, the partitioning between gas and aqueous phase concentrations of SO_2 are calculated. The calculation shows that without the consideration of aqueous phase reaction, the calculated gas-phase concentrations of SO_2 were significantly overestimated against the measured values (as indicated in the red lines of Fig. 9). For example, the measured concentrations of SO_2 during the 3 fog periods are about 5 ppbv, while the calculated concentrations are about 20 ppbv that is about 4 times higher than measured values. In contrast, when the S_{eff} value is applied in the calculation, the calculated SO_2 concentrations are significantly improved. For example, the calculated minimum concentrations of SO_2 are close to the measured values (as indicated in the blue lines of Fig. 9), showing significant reduction compared to the case when the aqueous phase reaction is not considered. Although the calculation with the S_{eff} value considerably improves the calculated concentrations of SO_2 during fog periods, there are still some discrepancies between the calculation and measurement. For instance, there is a tendency that the calculated SO_2 concentrations have an earlier increase (with a time lag of 2 h) compared to the measured values. In the calculation, the reduction of SO_2 concentration is mainly due to the appearance of LWC. Thus, any uncertainty of measured LWC could cause the errors in the calculation of SO_2 concentration during fog periods.

4. Summary

In this study, a field experiment was conducted in a heavily SO_2 polluted area in the NCP region. During the experiment, large variability of SO_2 and liquid water content (LWC) of fog droplets were observed, providing a good opportunity to study the solubility of SO_2.

Measurements were carried out for three fog periods occurring between November 5 and November 8, 2009, with averaged LWC of 0.23, 0.35, and 0.35 g/m^3, respectively. During the fog periods, the measured SO_2 concentrations showed strong variability which was found to be closely related to the appearance of fogs and variation of LWC. For example, the averaged concentration of SO_2 during the non-fog period was about 25 ppbv. In contrast, the concentrations of SO_2 during the 3 fog periods were significantly reduced to 6.8, 4.4, 7.2 ppbv, respectively. The large reduction of SO_2 concentrations suggests that SO_2 was significantly reduced by dissolving into fog droplets during the formation of the fogs. The large reduction of SO_2 (about 70%–80%) during the fog periods suggests that the solubility of SO_2 is considerably increased. However, calculation using effective Henry's Law constant significantly underestimates the gas to aqueous conversion of SO_2, and thus cannot explain the measured large reduction of gas-phase concentrations of SO_2. This result suggests that aqueous reactions of SO_2 play important roles to enhance the solubility of SO_2. Thus, an effective solubility coefficient of S_{eff} of SO_2 is proposed in this study, to account for the effect of aqueous reactions on the solubility of SO_2. The study shows that when the S_{eff} coefficient is applied in the calculation, the calculated SO_2 concentrations are significantly improved, showing that the aqueous reactions of SO_2 play important roles in controlling the solubility of SO_2, and should be considered in model calculations.

Acknowledgements

This research is partially supported by Basic Research Fund of CAMS (Chinese Academy of Meteorological Science) (2008Z011); National Natural Science Foundation of China (NSFC) under Grant Nos. 40905060 and 41275168; The National Basic Research Program of China (2006CB403701); Science and Technology Administration of China under Grant No. 2006BAC12B00. The National Center for Atmospheric Research is sponsored by the National Science Foundation.

References

Carmichael, G. R., & Peters, L. K. (1979). Some aspects of SO_2 absorption by water-generalized treatment. *Atmospheric Environment*, *13*, 1505–1513.

Chameides, W. L. (1984). The photochemistry of remote marine stratiform cloud. *Journal of Geophysical Research*, *89*, 4739–4755.

Chin, M., Rood, R. B., Lin, S. J., Müller, J. F., & Thompson, A. M. (2000). Atmospheric sulfur cycle simulated in the global model GOCART: model description and global properties. *Journal of Geophysical Research*, *105*, 24671– 24687.

Dutkiewicz, V. A., Burkhard, E. G., & Husain, L. (1995). Availability of H_2O_2 for oxidation of SO_2 in clouds in the Northeastern United States. *Atmospheric Environment*, *29*, 3281–3292.

Hoag, K. J., Collett, J. L., Jr., & Pandis, S. N. (1999). The influence of drop size-dependent fog chemistry on aerosol processing by San Joaquin Valley fogs. *Atmospheric Environment*, *33*, 4817–4832.

IEA. (2010). *Key world energy statistics*. Paris: International Energy Agency.

Kawamoto, K., Hayasaka, T., Nakajima, T., Streets, D., & Woo, J. H. (2004). Examining the aerosol indirect effect over China using an SO_2 emission inventory. *Atmospheric Research*, *72*, 353–363.

Kreidenweis, S. M., Walcek, C. J., Feingold, G., Gong, W. M., Jacobson, M. Z., Kim, C. H., et al. (2003). Modification of aerosol mass and size distribution due to aqueous-phase SO_2 oxidation in clouds: comparisons of several models. *Journal of Geophysical Research*, *108*, 4213. http://dx.doi.org/10.1029/2002JD002697

Malm, W. C., Trijonis, J., Sisler, J., Pitchford, M., & Dennis, R. L. (1994). Assessing the effect of SO_2 emission changes on visibility. *Atmospheric Environment*, *28*, 1023–1034.

Pandey, J. S., Kumar, R., & Devotta, S. (2005). Health risks of NO_2, SPM, and SO_2 in Delhi (India). *Atmospheric Environment*, *39*, 6868–6874.

Quan, J., Zhang, Q., He, H., Liu, J., Huang, M., & Jin, H. (2011). Analysis of the formation of fog and haze in North China Plain (NCP). *Atmospheric Chemistry and Physics*, *11*, 8205–8214.

Ravishankara, A. R. (1997). Heterogeneous and multiphase chemistry in the troposphere. *Science*, *276*, 1058–1065.

Ren, Y., Ding, A., Wang, T., Shen, X., Guo, J., Zhang, J., et al. (2009). Measurement of gas-phase total peroxides at the summit of Mount Tai in China. *Atmospheric Environment*, *43*, 1702–1711.

Seinfeld, J. H., & Pandis, S. N. (1998). *Atmospheric chemistry and physics: From air pollution to climate change*. New York: John Wiley and Sons.

Streets, D. G., & Waldhoff, S. T. (2000). Present and future emissions of air pollutants in China: SO_2, NO_x, and CO. *Atmospheric Environment*, *34*, 363–374.

Tang, J., Xu, X. B., Ba, J., & Wang, S. F. (2010). Trends of the precipitation acidity over China during 1992–2006. *Chinese Science Bulletin*, *55*, 1800–1807.

Tie, X., & Cao, J. (2009). Aerosol pollution in China: Present and future impact on environment. *Particuology*, *7*, 426–431.

Tie, X., Wu, D., & Brasseur, G. (2009). Lung cancer mortality and exposure to atmospheric aerosol particles in Guangzhou China. *Atmospheric Environment*, *43*, 2375–2377.

Wang, Y., Guo, J., Wang, T., Ding, A., Gao, J., Zhou, Y., et al. (2011). Influence of regional pollution and sandstorms on the chemical composition of cloud/fog at the summit of Mt Taishan in northern China. *Atmospheric Environment*, *99*, 434–442.

Zhang, Q., Ma, X. C., Tie, X., Huang, M., & Zhao, C. (2009). Vertical distributions of aerosols under different weather conditions: Analysis of in-situ aircraft measurements in Beijing China. *Atmospheric Environment*, *43*(34), 5526– 5535.

Zhao, C., Tie, X., & Lin, Y. (2006). A possible positive feedback of reduction of precipitation and increase in aerosols over eastern central China. *Geophysical Research Letters*, *33*, L11814.

Zhou, Y., Wang, T., Gao, X., Xue, L., Wang, X., Wang, Z., et al. (2009). Continuous observations of water-soluble ions in $PM_{2.5}$ at Mount Tai (1534 m a.s.l.) in central-eastern China. *Journal of Atmospheric Chemistry*, *64*(2), 107–127.